

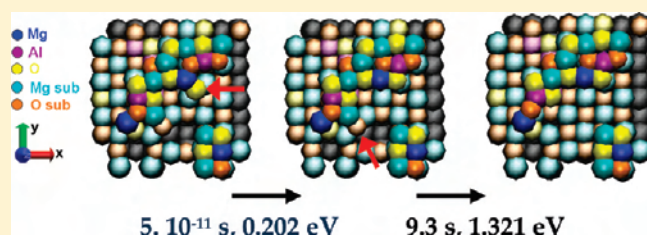
Understanding the Surface Diffusion Processes during Magnetron Sputter-Deposition of Complex Oxide Mg–Al–O Thin Films

Violeta Georgieva,^{*,†} Arthur F. Voter,[‡] and Annemie Bogaerts[†]

[†]Research Group PLASMANANT, Department of Chemistry, University of Antwerp (UA), Universiteitsplein 1, Antwerp B-2610, Belgium

[‡]Theoretical Division, T-1, MS B268, Los Alamos National Laboratory, Los Alamos, New Mexico 87545, United States

ABSTRACT: It is known that film structure may change dramatically with the extent of surface diffusion during the film growth process. In the present work, surface diffusion, induced thermally or activated by energetic impacts, is investigated theoretically under conditions appropriate for magnetron sputter-deposition of Mg–Al–O thin films with varying stoichiometry. The distribution of surface diffusion energy barriers available to the system was determined for each stoichiometry, which allowed assessing in a qualitative way how much surface diffusion will take place on the time scale available between deposition events. The activation energy barriers increase with the Al concentration in the film, and therefore, the surface diffusion rates in the time frame of typical deposition rates drop, which can explain the decrease in crystallinity in the film structure and the transition to amorphous structure. The deposition process and the immediate surface diffusion enhanced by the energetic adatoms are simulated by means of a molecular dynamics model. The longer-time thermal surface diffusion and the energy landscape are studied by the temperature accelerated dynamics method, applied in an approximate way. The surface diffusion enhanced by the energetic impacts appears to be very important for the film structure in the low-temperature deposition regime.



I. INTRODUCTION

Many new technologically interesting materials have a complex chemical and crystalline structure.¹ Complex metal oxide thin films belong to this class, and therefore, it is of considerable interest to investigate methods that allow deposition of such films with good control of the film composition as well as to study the relations between the film stoichiometry and film structure and properties.

Magnetron sputtering using individual metal targets can offer a good control of the film composition.^{2,3} Therefore, this method has been applied to grow Mg–M–O thin films (with M = Al, Cr, Ti, Y, and Zr) with varying stoichiometry.^{4,5} The growth of MgO thin films is well studied, and hence, this oxide was used as an initial material for research when another metal is added. Along with the experimental study, atomistic simulations of the thin film deposition, by means of classical molecular dynamics (MD), were carried out.^{5,6} Although two major simplifications were set into the developed MD model in order to make it effective in a reasonable CPU time (see below), the model predicted well the film structure for the systems for which reliable interatomic interaction potentials were available in the literature (M = Al, Cr, and Y). It was found that when adding the other metal M at low concentration, the structure of the film is MgO rock salt with M in solid solution. Increasing the M concentration decreased the crystallinity until at some point an amorphous structure was detected.^{5,6} Moreover, in the case of adding Y, Y₂O₃ nanocrystallites were found in the amorphous regions.⁷

In these earlier studies, two main approximations were implemented to make the MD modeling viable. First, the

deposited species were metallic and oxygen ions instead of neutral metallic atoms or oxygen molecules, although the neutral species typically have the major contribution in real film growth.^{8,9} This means that the simulation started with the chemisorbed states of the deposited ad-particles. Hence, the initial high mobility of the physisorbed metallic adatoms, which improves the film density by reducing void formation,¹⁰ was not simulated. Nevertheless, their energy contribution to the film was taken into account. In addition, the ad-particles reside in the chemisorbed stable state for a much longer time compared to the time they reside in the physisorbed metastable state.¹⁰ For example, in the case of deposition of MgO thin films, it was shown that the formation of a MgO diatomic molecule is the basic charge-transfer process and the molecule is indeed a stable entity with a very long lifetime.¹¹ Moreover, it was calculated that the process does not have an activation barrier, except for diffusion of the Mg adatom (~ 0.3 eV); i.e., the process has high reaction rates, and the mobile Mg adatoms form ionic bonds shortly after their deposition if enough oxygen is deposited too.¹¹

The second approximation in the MD simulations was related to the time between two impacts in the deposition process. In the developed MD model, two successive impacts in the deposition process were carried out on a time scale of picoseconds, whereas in reality the time between impacts is on the order of milliseconds,

Received: March 14, 2011

Revised: April 8, 2011

Published: April 11, 2011

for typical experimental deposition rates of 10–100 nm/min. It was felt that this assumption was more or less justified, because there was enough time between successive depositions to allow quick surface diffusion events stimulated by the excess energy from the deposition process. The thermally activated diffusion events, which might take place on the longer time scales, are expected to have fairly high barriers, so their contribution to the overall film morphology might not be very strong.

In the present work, we take a step toward quantifying the importance of the long-time diffusive events during the deposition of these films, i.e., events that were omitted in the studies described above. Using an accelerated molecular dynamics approach, we directly simulate the long-time (ms) dynamics after every few deposition events, to allow some surface diffusion to take place during the film growth. Moreover, we determine the distribution of surface diffusion energy barriers available to the system, which allows us to assess in a qualitative way how much surface diffusion will take place on the time scale available between deposition events. This is done for Mg–Al–O films with varying stoichiometry. In particular, we are interested in understanding the transition from crystalline to amorphous film structure as the Al content is increased, a transition that was observed both experimentally and in our previous MD simulations.⁶

MD simulations follow the exact dynamic evolution of the system, with time steps on the order of femtoseconds. Even using currently available computer power, the MD simulations rarely reach a “real time” greater than hundreds of nanoseconds. The simulated time scale of MD simulations can be successfully extended by one of the accelerated molecular dynamics methods.¹² We have chosen the temperature accelerated dynamics (TAD) method,¹³ because it explores the energy landscape and it does not require an *a priori* list of all possible events, in contrast to, for instance, the kinetic Monte Carlo method. Indeed, creating such a list in advance is not a trivial task in the case of nonideal crystalline surfaces. The idea of the TAD method is to describe the system evolution based on infrequent events, as a sequence of transitions between distinct states. Surface diffusion in solids at low temperature is an example of infrequent events that take place on a time scale much longer than the atomic vibration period, e.g. order of millisecond and longer, and hence hardly can be simulated by the MD method. The TAD method simulates the thermal surface diffusion by state-to-state transitions, based on the activation energy barriers computed for events discovered at high temperature. By coupling the TAD method with the MD model for deposition, the surface diffusion can be accounted for in the simulations.

The paper is organized as follows. In the next section, the MD and TAD methods used in our simulation model are explained. Several examples of calculated activation energies for diffusion are presented in section III. A comparison of the film structures simulated by the MD model and by the coupled MD and TAD models is shown as well. In section IV the activation energy barrier distributions for surface diffusion during the deposition of films with different metal ratios (i.e., 100, 80, 60, 50, and 40% Al) are presented and discussed. We find that adding Al introduces defects in the structure of MgO (Mg vacancies) and, hence, the diffusion cannot be explained only by the basic atomistic mechanisms, such as hopping, exchange, and vacancy migration, as observed on an ideal crystalline surface. More complex rearrangements have been noticed, and therefore, we explored the energy landscape during the deposition of one monolayer with different stoichiometries. Finally, conclusions are given in section V.

II. DESCRIPTION OF THE MD AND TAD METHODS

The developed MD model for simulation of thin film growth has been presented in detail elsewhere.⁶ The MD package DL_POLY¹⁴ is used to simulate the deposition of atoms. A driving program is written, which automates the deposition and relaxation. The reliability of the MD results is largely determined by the interatomic potential used in the simulations.¹⁵ In the present study a classical two-body ionic potential¹⁶ describes the interactions between atoms. It has been demonstrated that this potential yields good agreement with the experiments for the structure of deposited Mg(M)O thin films (with M = Al, Cr, and Y).^{5,6,15} The initial crystalline or amorphous substrate cell has dimensions of $(1.7 \times 1.7 \times 1.7) \text{ nm}^3$. The metal or oxygen ions are deposited one by one. The initial velocities of the O^{2-} ions are sampled from a Maxwellian distribution with a most probable energy of 0.025 eV (300 K) and random direction. The velocities of Mg^{2+} and Al^{3+} ions have values calculated from a Maxwellian distribution with a most probable energy of 1 eV and a direction at a certain angle, corresponding to the position of the two metallic targets in the experiment where the sputtering occurs.⁶ More details on the developed MD model to simulate the film growth, potential parameters, and operating conditions for the Mg–Al–O system can be found in ref 6.

The TAD method, which is described in detail elsewhere,¹³ accelerates the diffusion by heating the system for a short time to obtain a sample of the possible diffusion pathways out of the current state (energy basin) of the system. Utilizing the harmonic transition state theory approximation, each of the escape times for the pathways discovered at the high temperature can be mapped onto a (longer) escape time at the lower (original) temperature. This requires knowing the energy barrier for each of these pathways; the saddle points are found using the nudged elastic band method.¹⁷ After a small number of these attempted escapes have been generated, the high temperature MD can be terminated, and the event with the shortest time at low temperature can be accepted. Given the additional assumption of a specific lower bound on the pre-exponential factors, a confidence level can be assigned to the statement that the accepted low-temperature event is the correct one, in the sense that running further MD at high temperature would not reveal a shorter-time event to replace it. In this way, the TAD method filters out some of the high-temperature transitions and allows only those transitions that should occur at the original temperature.

The TAD model can be successfully used for ordered systems. In the case of disordered systems, the number of very low energy barriers increases substantially, which increases the CPU time greatly, making the method ineffective for extension of the simulation time scale. Therefore, a crystalline MgO (100) structure is used as the substrate. The initial substrate system consists of 512 Mg and O ions, so that the dimension in each direction is at least twice the cutoff radius of 0.8 nm and the surface is simulated in 3D periodic boundary conditions by adding vacuum slabs.⁶

The MD and TAD models are coupled in the following way. First, the deposition is simulated by the MD method; subsequently, the dynamics are advanced using the TAD method. The TAD approach has been applied successfully to extend the simulation time and reproduce realistic experimental deposition rates for studying crystal growth at low temperatures.^{18,19} The method yielded significant boosts, but these were studies at very low temperatures (~ 70 – 80 K), and in metal systems with short-range interatomic potentials.^{18,19} In the present study, due to the substantially higher original temperature (500 K) and the more

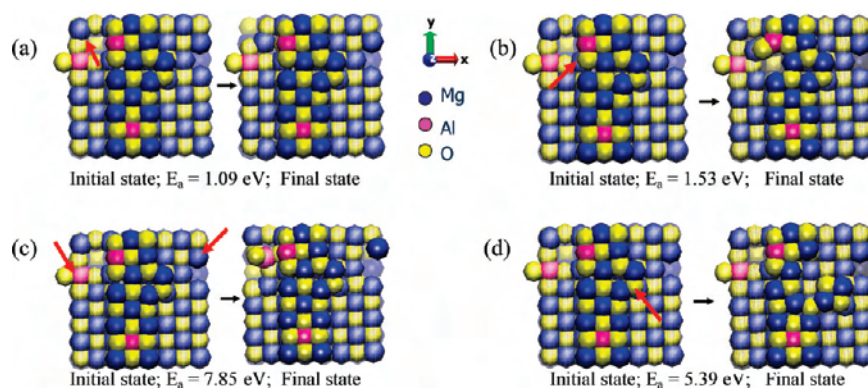


Figure 1. Examples of activation energy barriers for surface diffusion, as calculated by the TAD method. The atoms in the deposited layer are shown in full colors, the atoms from the surface layer are shown in weaker colors, and the atoms from the subsurface layer are presented in semitransparent colors. The red arrows show which atom or group of atoms move. The initial and final states are presented for migration of a Mg ion from the surface layer to a vacancy, with calculated E_a of 1.09 eV (a); for diffusion of a MgO dimer (i.e., Mg from the surface layer and O on top of it), with calculated E_a of 1.51 eV (b); for diffusion of an Al ion to a vacancy and displacement of the neighboring Mg and O, with calculated E_a of 7.85 eV (c); and for diffusion of $(\text{MgO})_2$ from the deposition layer, with E_a of 5.39 eV (d). The color code of the different atom types and the surface orientation is shown in the legend.

expensive long-range ionic potential, advancing the TAD dynamics required considerable computational investment when the surface diffusion barriers were low, as was the case for some stoichiometries. Therefore, directly accelerating the dynamics was difficult and the following approximation was implemented in order to apply the TAD method in a somewhat limited way. The TAD method was switched on after every 10 successive depositions in order to reduce substantially the computational time compared to the case when the TAD method is switched on after each deposition. It was difficult to follow a specific deposition rate in each case, but the time between depositions was extended far beyond the picosecond time scale. We also reduced the computational intensity by considering only the top five monolayers by the TAD method, and only the ions of the top two monolayers and the deposition layer are allowed to move in order to simulate the surface diffusion.

Our overall goal in this work was to obtain a qualitative understanding of the importance of activated diffusion events. Therefore, we used the potential of the TAD technique to explore the energy landscape by the following simulation experiment. We applied the combined MD and TAD model to deposit 64–70 atoms, which are the number of atoms in one monolayer, and scan for different surface diffusion events. The corresponding activation energy barriers were calculated. The TAD simulations were evolved for a time scale of seconds or until 100 transitions were observed, using an original temperature $T = 500$ K (see above) and a high temperature $T = 5000$ K. This was carried out for different metal ratios, and the activation energy barrier distribution was calculated for each stoichiometry.

III. CALCULATED ACTIVATION ENERGY BARRIERS FOR SURFACE DIFFUSION

The formation of a MgO diatomic molecule (dimer) plays a major role in the MgO film growth.¹¹ We reported¹⁵ that both the diffusion mechanisms for hopping and the interlayer exchange of Mg and O ions when one MgO dimer is deposited on the MgO(100) surface, as well as the corresponding activation energy barriers, calculated using the classical potential with formal charges,²⁰ were in reasonable agreement with the mechanisms and activation energy barriers calculated by a DFT study.²¹

Therefore, this classical potential is expected to describe the interactions correctly, not only in the bulk region for which the parameters have been fitted but also on the surface, where the film growth takes places. Indeed, the simulated film structure was found to be in excellent agreement with the structure of the experimentally deposited films.^{6,15}

The calculated energy barriers for hopping and interlayer exchange of Mg and O ions on a MgO(100) surface, when one MgO dimer was deposited, were found to be on the order of 0.3–0.5 eV.¹⁵ The activation barriers depend on the number of bonds that have to be broken and, hence, on the type and the number of the neighboring atoms. Adding Al to Mg and O introduces defects in the MgO structure, and hence, the diffusion cannot be explained only by the basic atomistic mechanisms, i.e. hopping, interlayer exchange, or vacancy migration, observed on an ideal crystalline surface. Indeed, more complex rearrangements were observed. We make no attempt to present an exhaustive list of all possible events for the Mg–Al–O system in this paper. In Figure 1 four possible transitions are illustrated by their initial and final state, as obtained by the TAD method. The corresponding energy barriers are shown as well. The atoms in the deposited layer are presented by full colors, the atoms occupying the surface layer are presented by weaker colors, and the atoms from the subsurface layer are presented by semitransparent colors. The activation energy barrier for diffusion of Mg to a vacancy was calculated to be on the order of 1 eV (Figure 1a), while the activation energy for diffusion of a MgO dimer was calculated to be 1.53 eV (Figure 1b). Migration of Al to a vacancy and displacement of the neighboring Mg and O have activation energy barriers of 7.85 eV (Figure 1c), while diffusion of $(\text{MgO})_2$ requires an activation energy of 5.39 eV (Figure 1d).

In order to diffuse, the surface atoms have to break chemical bonds on the order of typically 1–10 eV.²² The waiting time for a transition with an energy barrier of 1 eV is on the order of milliseconds for a substrate temperature of 500 K. Therefore, when simulating the film growth, only the diffusion processes with activation energy barriers below 1 eV are likely to be observed between two successive impacts in the millisecond time scale. In the experiment, the thin film grows at a typical deposition rate of 10–100 nm/min. Hence, one monolayer is deposited during 10–100 ms, and only a few basic diffusion

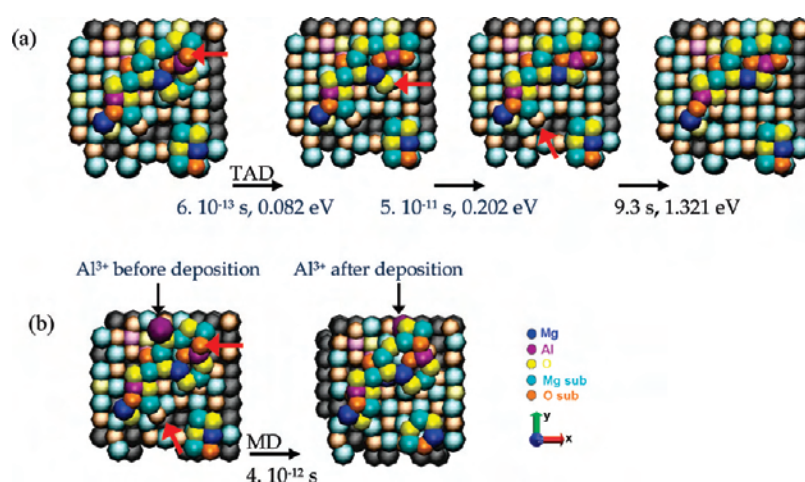


Figure 2. Thermal surface diffusion simulated by the TAD model (a). Snapshots of the initial, intermediate and final states are shown with the corresponding waiting times and energy barriers. The event at 9.3 s was well beyond the time for the next deposition and, hence, was not accepted. The surface diffusion on the same surface structure, but initiated by the impact of an Al ion with an initial energy of 1 eV, was also simulated by the MD model (b). The initial and final states are shown along with the simulated time. The atoms in the deposited layer are shown in full colors, the atoms from the surface layer are shown in weaker colors, and all the underlying atoms are presented in gray color. The red arrows show which atom or group of atoms move.

events will be observed before the next monolayer is deposited, unless the diffusion is enhanced locally by energetic impacts as in magnetron sputter-deposition. The MD method can simulate the diffusion events enhanced by the energetic adatoms because the adatom induced displacements are completed in just a few picoseconds after the impacts, as discussed above. The TAD model, on the other hand, simulates the thermally activated surface diffusion.

Figure 2 presents examples of thermal surface diffusion simulated by the TAD method (a), as well as the short-time diffusion enhanced by the deposition of one Al ion with an initial energy of 1 eV, as obtained by the MD method (b). The arrows show which atom, or atoms, are displaced during the simulation. The inter- and intralayer displacements are found to be very similar during the thermal or energy-induced diffusion. However, the time scale for the thermally activated surface diffusion is much longer (i.e., order of \sim s) compared to the time scale for the energy-induced diffusion (i.e., order of \sim ps). Since the time between two impacts is on the millisecond time scale, the last transition in Figure 2a would not be observed if there would be no additional energy supply to the surface. This means that the surface diffusion, enhanced locally by the highly energetic metal ad-atoms or by impacts of energetic ions from the plasma, is very important for the film structure in the low-temperature deposition regime, where thermally activated processes are exponentially suppressed. Similar conclusions were drawn from the simulation of Pt thin film growth by the deposition of hyperthermal Pt atoms.^{23,24}

As mentioned above, we combined the MD and TAD models so that the simulation time between deposition events simulated by the MD model could be extended far beyond the picosecond time scale. Due to the high original temperature and complex system under study, it is difficult to follow the exact deposition rates. The approximations set in the combined MD+TAD model (see section II) allowed us to simulate the deposition of a film with sufficient thickness (i.e., 15 monolayers) to calculate the radial distribution functions (RDFs) for the bulk film in a

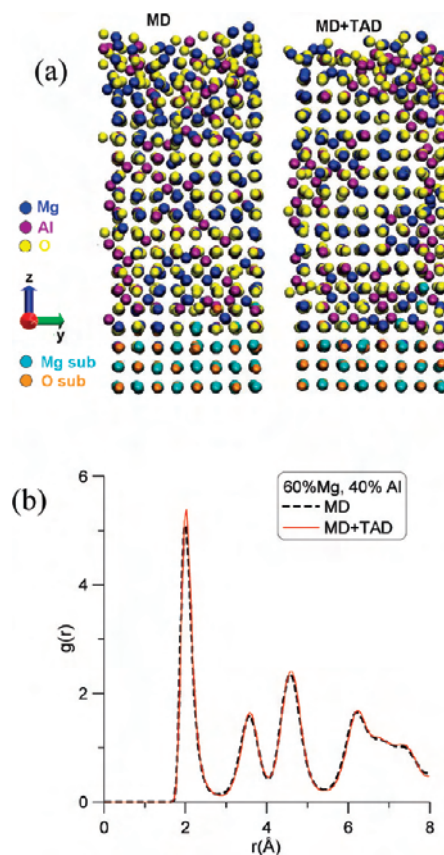


Figure 3. Snapshots (a) of thin film deposition at 60% Mg and 40% Al metal ratio on a MgO (100) crystal substrate, simulated by the MD model and by the combined MD+TAD method. The color legend is shown. The corresponding Mg–O RDFs are shown in part b.

reasonable computational time. Only a very small difference was observed in the film structure between the simulations performed with the MD method and the combined MD+TAD

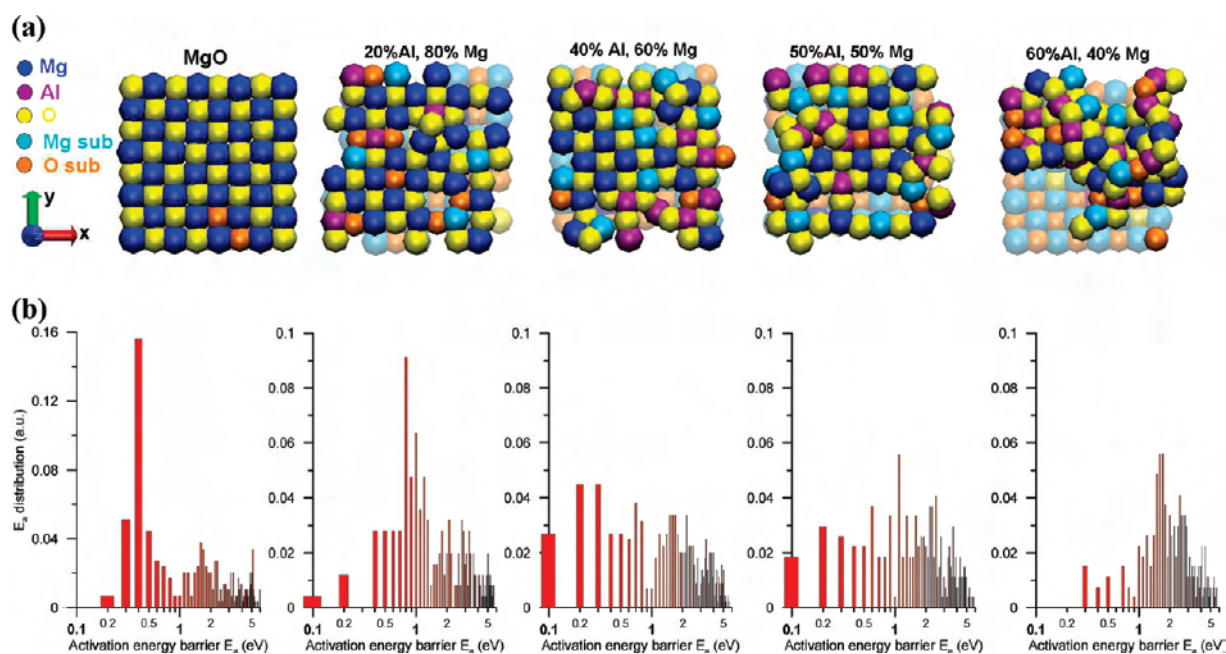


Figure 4. Snapshots of the final state after deposition of 64–70 atoms with different ratios of Mg and Al (a). The atoms in the deposited layer are shown by full colors, and the atoms in the surface layer are presented by semitransparent colors. In part b the distribution of the activation energy barriers is presented, calculated by sampling events with TAD at $T = 5000$ K during the deposition of one monolayer of Mg–Al–O film for the Mg/Al metal ratios shown in part a.

method, in which some long-time thermally activated diffusion was allowed. Snapshots of the films deposited only by the MD model and by the combined MD+TAD method are shown in Figure 3 along with the calculated RDFs. In order to calculate the RDF, the central part of the film is cut, so that the bottom three layers close to the substrate and the top three layers close to the free surface are excluded. Only the Mg–O RDFs are illustrated, since all the other pair RDFs showed the same trend. It is clear that the two functions have very similar profiles. This leads us to conclude indeed that the simulation of the thermally activated surface diffusion in the typical time scale of deposition of one monolayer has no influence on the film structure because of its low rate. Hence, the fast deposition in the developed MD model could be safely accepted. However, the TAD technique can be used as a powerful tool to scan the possible diffusion mechanisms (see Figures 1 and 2) and produces extremely interesting results, as is shown also in the next section.

IV. ACTIVATION ENERGY BARRIER DISTRIBUTION AT DIFFERENT FILM STOICHIOMETRIES

One of the main aims of our study was to elucidate the mechanisms behind the transition from crystalline to amorphous structure in Mg–Al–O films when the Al concentration increases. Because we expected that this mechanism is related to surface diffusion, we have calculated the activation energy barriers for surface diffusion for several Mg–Al–O films, with varying Al concentration. More specifically, we have studied the distributions of activation energy barriers, in order to obtain some statistically meaningful results.

Since the activation energy barriers depend on the number of neighboring atoms, the deposition of one monolayer was investigated, so that as many as possible different configurations would be studied. The energy landscape during the deposition of

64–70 atoms was investigated, and the activation energy barrier distribution with a step of 0.1 eV was calculated for several Mg–Al–O films. The following film stoichiometries were considered: pure MgO, as well as Mg–Al–O films with 20, 40, 50, and 60% metal ratios of Al. The film with 60% Al was found to be amorphous,⁶ and therefore, films with higher concentration of Al were not studied. Snapshots of the final states (top view) are illustrated in Figure 4a. The corresponding distribution of the energy barriers is presented in Figure 4b. The perfect coverage and crystal structure in the case of MgO deposition is clearly observed. Adding Al decreases the coverage and initiates the formation of defects (Mg vacancies) in the MgO crystal structure. Furthermore, it is observed that the maximum in the energy barrier distribution shifts to higher energy. This could be explained by the addition of another atom type, which is bonded more strongly, as well as by the formation of defects, which creates an imperfect energy surface. Indeed, the Al^{3+} ion has a higher charge than the Mg^{2+} ion, and hence, it is bonded more strongly to the surface, taking into account that the Coulomb energy contribution to the total configurational energy in ionic systems is an order of magnitude higher than the short-range energy contribution,²⁵ as was also observed in our calculation results.

When a pure MgO film is deposited, the activation energy barriers were found to be low and the maximum of their distribution was observed at 0.4 eV (Figure 4b). Hence, the surface diffusion rate is high, even at the low substrate temperature, and this explains the high degree of crystallinity of the MgO film structure found both in the simulations and in the experiment.⁶ At 20% Al, the maximum shifts to 0.8 eV, and a further increase of the Al content spreads considerably the distribution, showing more and more activation energy barriers larger than 1 eV. At 60% Al, the maximum of the distribution is found at 1.6 eV. Therefore, the degree of surface diffusion, both

thermally activated at the substrate temperature of 500 K under study, and locally activated by the energetic adatoms, decreases substantially. Consequently, the crystallization is quenched by lowering considerably the surface diffusion rate in the time frame until the next layer would be deposited; that is, the degree of crystallinity decreases and an amorphous structure is observed.⁶

V. CONCLUSIONS

In this work, an MD model for the atomistic simulation of thin film growth was combined with the TAD method to extend the simulation time scale and consider the thermal surface diffusion during the simulation of complex oxide thin film growth. Because of the high original temperature and complex system under study, the real experimental deposition rates were not achieved. Nevertheless, the TAD method gave valuable information on the surface diffusion mechanisms and their activation energy barriers.

Two types of activation of the surface diffusion, i.e. thermally and activated by energetic impact, were demonstrated. The MD method can simulate the diffusion events enhanced by the energetic adatoms because the adatom induced displacements are completed in just a few picoseconds after the impacts. The TAD model, on the other hand, simulates the thermally activated long-time-scale surface diffusion. It was shown that the immediate surface diffusion activated by the energetic impacts has much higher rates than the thermally activated long-time-scale surface diffusion, which is exponentially suppressed in the low-temperature magnetron sputter deposition regime.

Finally, in order to elucidate the mechanisms behind the transition from crystalline to amorphous structure in Mg–Al–O thin films when the Al concentration increases, the energy landscape during the deposition of one monolayer was investigated and the activation energy barrier distributions were calculated for Mg–Al–O films with different stoichiometries. The calculated activation energy barriers for diffusion increase with the increase of Al concentration in the films, and therefore, the surface diffusion rates decrease. Consequently, the crystallization is quenched by lowering the surface diffusion rate in the time frame until the next layer would be deposited. Hence, this can explain the observed decrease in crystallinity in the film structure and the transition to amorphous structure in Mg–Al–O films at increasing Al concentration.

AUTHOR INFORMATION

Corresponding Author

*E-mail address: violeta.georgieva@ua.ac.be.

Funding Sources

This work is supported by the IWT-Flanders (SBO project). Calculations have been performed on the CALCUA super-computer of the University of Antwerp and on the FISTUA computer facilities of the PLASMANT research group. Work at Los Alamos National Laboratory (LANL) was funded by the Office of Science, Office of Basic Energy of Sciences, Division of Materials Science. LANL is operated by Los Alamos National Security, LLC, for the National Nuclear Security Administration of the U.S. DOE under Contract No. DE-AC52-06NA25396.

ACKNOWLEDGMENT

V.G. would like to thank B. P. Uberuaga for his help and support in getting familiar with the TAD code. The authors are

grateful to N. Jehanathan, G. Van Tendeloo, D. Depla, and M. Saraiva for the helpful discussions and comparison to the experiments.

REFERENCES

- (1) Willmott, P. R. *Prog. Surf. Sci.* **2004**, 76, 163–217.
- (2) Berg, S.; Nyberg, T. *Thin Solid Films* **2005**, 476, 215–230.
- (3) Martin, N.; Rousselot, C. *Surf. Coat. Technol.* **1999**, 114, 235–249.
- (4) Saraiva, M.; Chen, H.; Leroy, W. P.; Mahieu, S.; Jehanathan, N.; Lebedev, O.; Georgieva, V.; Persoons, R.; Depla, D. *Plasma Process. Polym.* **2009**, 6, S751–S754.
- (5) Saraiva, M.; Georgieva, V.; Mahieu, S.; Van Aeken, K.; Bogaerts, A.; Depla, D. *J. Appl. Phys.* **2010**, 107, 034902.
- (6) Georgieva, V.; Saraiva, M.; Jehanathan, N.; Lebedev, O. I.; Depla, D.; Bogaerts, A. *J. Appl. Phys.* **2009**, 42, 06S107.
- (7) Jehanathan N.; Georgieva, V.; Saraiva, M.; Depla, D.; Bogaerts, A.; Van Tendeloo, G. Accepted for publication in *Thin Solid Films* 2011, doi: 10.1016/j.tsf.2011.02.050.
- (8) Depla, D., Mahieu, S., Eds.; *Reactive Sputter Deposition*; Springer Series in Materials Science; 2008; Vol. 109.
- (9) Vancoppenolle, V.; Jouanb, P.-Y.; Ricard, A.; Wauteleta, M.; Dauchota, J.-P.; Hecqa, M. *Appl. Surf. Sci.* **2003**, 205, 249–255.
- (10) Smith, D. L. *Thin-film deposition: Principles and practice*; McGraw-Hill, Inc.: 1995.
- (11) Geneste, G.; Morillo, J.; Finocchi, F.; Hayoun, M. *Surf. Sci.* **2007**, 601, S616–S627.
- (12) Voter, A. F.; Montalenti, F.; Germann, T. C. *Annu. Rev. Mater. Res.* **2002**, 32, 321–346.
- (13) Sorensen, M. R.; Voter, A. F. *J. Chem. Phys.* **2000**, 112, 9599–9606.
- (14) Todorov, I. T.; Smith, W.; Trachenko, K.; Dove, M. T. *J. Mater. Chem.* **2006**, 16, 1611–1618.
- (15) Georgieva, V.; Todorov, I. T.; Bogaerts, A. *Chem. Phys. Lett.* **2010**, 485, 315–319.
- (16) Catlow, C. R. A.; Freeman, C. M.; Royle, R. L. *Physica* **1985**, 131B, 1–12.
- (17) Henkelman, G.; Uberuaga, B. P.; Jónsson, H. *J. Chem. Phys.* **2000**, 113, 9901–9904.
- (18) Montalenti, F.; Sorensen, M. R.; Voter, A. F. *Phys. Rev. Lett.* **2001**, 87, 126101.
- (19) Sprague, J. A.; Montalenti, F.; Uberuaga, B. P.; Kress, J. D.; Voter, A. F. *Phys. Rev. B* **2002**, 66, 205415.
- (20) Bacorisen, D.; Smith, R.; Ball, J. A.; Grimes, R. W.; Uberuaga, B. P.; Sickafus, K. E.; Rankin, W. T. *Nucl. Instrum. Methods Phys. Res., Sect. B* **2006**, 250, 36–45.
- (21) Henkelman, G.; Uberuaga, B. P.; Harris, D. J.; Harding, J. H.; Allan, N. L. *Phys. Rev. B* **2005**, 72, 115437.
- (22) Oura, K.; Lifshits, V. G.; Saranin, A. A.; Zotov, A. V.; Katayama, M. *Surface Science: An Introduction*; Springer-Verlag: Berlin Heidelberg, 2003.
- (23) Adamovic, D.; Munger, E. P.; Chirita, V.; Hultman, L.; Greene, J. E. *Appl. Phys. Lett.* **2005**, 86, 211915.
- (24) Adamovic, D.; Chirita, V.; Munger, E. P.; Hultman, L.; Greene, J. E. *Phys. Rev. B* **2007**, 76, 115418.
- (25) Gale, J. D. *Philos. Mag. B* **1996**, 73, 3–19.